ELSEVIER

Surface Science 343 (1995) L1151–L1155

surface science

Surface Science Letters

Velocity distributions of recombinatively desorbed O_2 originating from surface and sub-surface oxygen/Rh(111)

K.D. Gibson, J.I. Colonell, S.J. Sibener *

The James Franck Institute and The Department of Chemistry, The University of Chicago, 5640 South Ellis Avenue, Chicago, IL60637, USA

Received 12 July 1995; accepted for publication 17 August 1995

Abstract

Oxygen can exist either on the surface or in the sub-surface region of Rh(111). There are clearly different thermal desorption signatures for these two states. In this Letter, we report on experiments examining the dynamical paths for oxygen recombination and desorption arising from the two states by measuring the velocity distributions of the desorbing O_2. The results are well represented by *identical* Maxwell–Boltzmann velocity distributions, significantly hotter than the surface temperature. We conclude that surface and sub-surface oxygen share a common dynamical state prior to desorption.

Keywords: Adsorption kinetics; Atom–solid reactions; Low index single crystal surfaces; Molecule–solid reactions; Oxygen; Rhodium; Surface chemical reaction; Thermal desorption

1. Introduction

Much is known about the interactions of oxygen with the Rh(111) surface. At elevated surface temperatures, certainly above 200 K, oxygen is dissociatively adsorbed, with a saturation coverage of 0.5 monolayers (ML) [1,2]. Two ordered structures are observed, at 0.25 and 0.5 monolayers [2–4]. These both exhibit (2×2) diffraction patterns, due to a (2×2) overlayer at 0.25 ML, and due to rotated (2×1) domains at 0.5 ML. He diffraction measurements indicate that these structures can exist to at least $T_s = 525$ K [3–5]. With continued exposure at $T_s \geqslant 400$ K, oxygen is also absorbed into the sub-surface region at an appreciable rate [3,6]. Temperature programmed desorption (TPD) experiments, where the temperature of the surface is ramped while measuring the intensity of desorbed oxygen, shows that the desorption of 0.5 ML of surface adsorbed oxygen occurs over a wide temperature range, ~650–1250 K. In contrast to this, the sub-surface oxygen desorbs predominately in a sharp peak over a very narrow temperature range. Therefore, there is a clear signature of when much of the absorbed oxygen leaves the selvedge. We used this observation to ascertain whether there is a difference in the dynamical paths for gas phase O_2 originating from the recombination of surface and sub-surface oxygen atoms. This was accomplished by comparing the time-of-flight (TOF) spectra of O_2 desorbing from a crystal with 0.5 ML of surface oxygen and O_2 desorbing from a crystal having both adsorbed and absorbed oxygen in the initial state.

* Corresponding author. Fax: +1 312 702 5863; E-mail: Sibener@silly.uchicago.edu.

SSDI 0039-6028(95)00895-0

Comparable experiments exist for hydrogen and deuterium. TOF measurements have been done for D_2 and H_2 desorbing from Ni and Cu single crystals, after permeation of the atoms through the bulk [7,8]. The results can be rationalized with dissociative adsorption measurements through the principle of detailed balance [9–12]. It therefore appears that the atoms permeate to the surface where they reach local equilibrium, recombine, and desorb. However, there are examples of differing surface chemistry when atoms are adsorbed or absorbed. Hydrogen atoms, formed by thermal dissociation of H_2 on a hot filament, can be absorbed into Ni under UHV conditions [13]. These atoms can then hydrogenate CH_3 and C_2H_4, something that adsorbed H cannot accomplish [14,15].

2. Experimental

These experiments were performed in a scattering machine more thoroughly described elsewhere [16,17]; only the essential features will be mentioned here. The UHV scattering chamber has a differentially pumped quadrupole mass spectrometer with an angular resolution of 1°. Attached to the detector housing is a doubly differentially pumped housing containing an AC hysteresis motor for driving a post-crystal chopper with a 511 channel cross-correlation pattern, spinning at 195.69 Hz (10 μs/channel). This chopper interrupts the O_2 desorbing from the Rh(111) crystal at a distance of 10.5 cm from the electron impact ionizer. Detection was done normal to the crystal surface.

Room temperature molecular beams of both O_2 and NO_2 were used to dose the crystal with oxygen. NO_2 was used because it decomposes and deposits oxygen more readily than an O_2 beam [3]. For absorbing large quantities of oxygen, we dosed the crystal for up to an hour at $T_s = 650$ K. For the TPD spectra, we grew a saturation coverage of 0.5 ML by exposing the crystal to the O_2 beam for 20 min at $T_s = 300$ K. It was found that an exposure to this same beam for 5 min at $T_s = 450$ K gave saturation coverage with <0.1 ML of oxygen in the bulk; this dosing procedure was used for the TOF experiments. TPD spectra were taken at a ramp rate of 10 K/s, using the same detector as was used for the TOF measurements. The quantity of oxygen ad- and absorbed was determined by comparing the total integrated TPD signal with that of the saturated 0.5 ML state. The precision of the coverage measurements is about ±0.1 ML.

For 0.5 ML of adsorbed oxygen, the TOF measurements were made while ramping the surface temperature up to 1250 K at 10 K/s. The TOF measurements for the sub-surface oxygen were taken while ramping the temperature at 10 K/s, terminating at a temperature just above the position in the TPD spectra of the sharp peak due to the presence of absorbed oxygen. Each experiment was repeated several times, and the results added together to enhance the signal-to-noise ratio. During the experiments with both surface and sub-surface oxygen, some of the surface oxygen desorbed, but <0.25 ML, so the spectra are dominated by desorption due to sub-surface oxygen.

3. Results

Fig. 1 shows a comparison of some oxygen TPD spectra taken with varying amounts of sub-surface oxygen. Fig. 1b shows results when O_2 was used for dosing, and Fig. 1c shows results when NO_2 was used. For all dosing conditions oxygen desorbs over a wide temperature range, continuing until the surface reaches ~1250 K. This is shown in Fig. 1a for 0.5 ML of adsorbed oxygen. The entire desorption spectra are not shown in Figs. 1b and 1c so that we can present an expanded view of the desorption peaks due to sub-surface oxygen. Clearly, for both O_2 and NO_2 dosing, there is a systematic shift of the peaks to higher temperature as the quantity of sub-surface oxygen increases. A second significant feature is that, for equivalent quantities, desorption of sub-surface oxygen occurs at a higher temperature when deposited using NO_2 rather than O_2. To determine whether the difference might be due to co-absorbed nitrogen, we also looked for NO and N_2 desorbing after NO_2 dosing, but were unable to detect any. In the case of N_2, however, our relative sensitivity is low because of the high $m/e = 28$ background in our

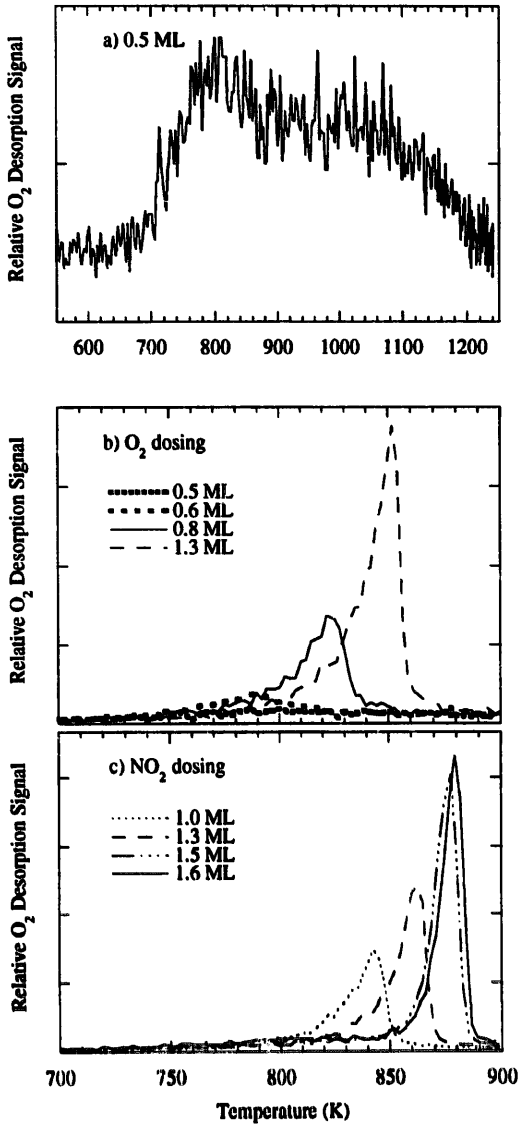

Fig. 1. TPD spectra of O_2 desorbing from Rh(111), with a ramp rate of 10 K/s. (a) Shows the results for a saturation coverage of 0.5 ML of adsorbed oxygen. The ramp rate is slowing near the end of the spectrum, thus the greater density of points. (b) Shows the results for varying amounts of ad- and absorbed oxygen deposited by O_2 dosing, and (c) shows some results when NO_2 was used to deposit the oxygen.

detector. The desorption of N_2 from the decomposition of NO adsorbed on Rh(111) has been observed to occur below the temperature at which sub-surface oxygen desorption occurs in our spectra [18–20]. The desorption of nitrogen deposited on the surface with an N atom source has also been investigated [21], and the desorption temperature is again lower than we observed for the desorption of sub-surface oxygen. However, in none of these experiments was the crystal dosed at as high a surface temperature as was used here.

Fig. 2 shows TOF spectra for desorbed O_2 arising from three different amounts of dosed oxygen; in all three cases an O_2 beam was used to deposit the oxygen. These include desorption of 0.5 ML of

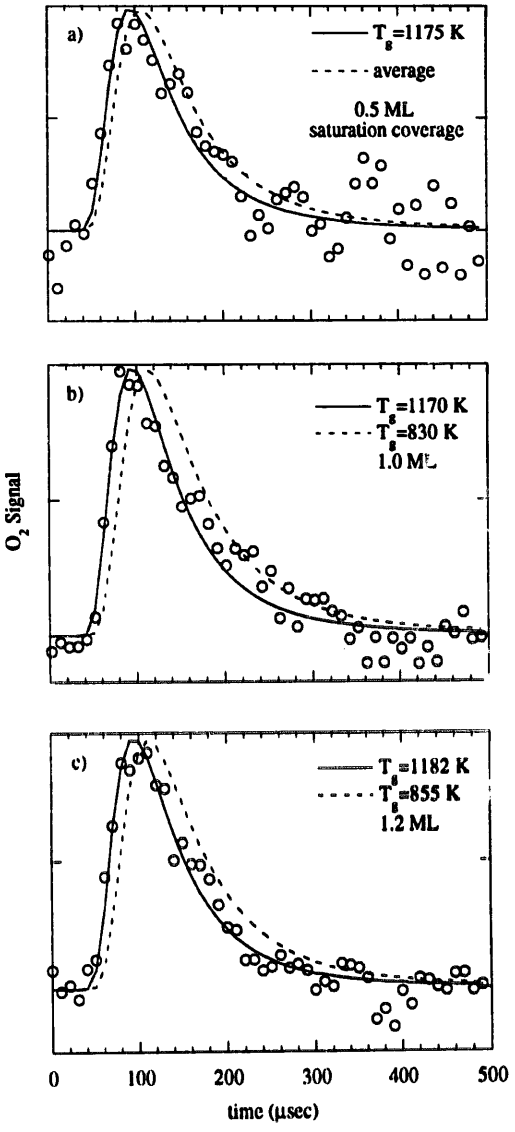

Fig. 2. Deconvoluted O_2 TOF spectra (circles) and least squares fits (lines) for varying amounts of ad- and absorbed oxygen, all taken after O_2 dosing. The dashed line for 0.5 ML of adsorbed oxygen (a) is what would be expected if the O_2 were desorbing at the surface temperature of the crystal (see text). The dashed lines in (b) and (c) are expected TOF spectra for the surface temperature at which most of the desorption occurs for the given amount of oxygen.

surface adsorbed oxygen (Fig. 2a), and desorption of a mixture of surface and sub-surface oxygen, a total of 1.0 ML (Fig. 2b) and 1.2 ML (Fig. 2c). To arrive at the results shown, we took the cross-correlation data collected from successive runs and added them together. The raw data was then smoothed by a running three-point average; averaging each point with its two nearest neighbors. The smoothed spectra were then deconvoluted from the cross-correlation sequence, with the result shown by the circles in Fig. 2. Each solid line is from a nonlinear least squares fit using a Maxwell–Boltzmann velocity distribution,

$$f(v) \propto v^3 \exp\left(\frac{-m_g v^2}{k_b T_g}\right) \qquad (1)$$

(where m_g is the mass of a gas atom, k_b is Boltzmann's constant, and T_g is the temperature of the gas molecules), convoluted with the instrumental broadening due to the finite length of the ionizer. The resulting best fit values of T_g are 1175 K for 0.5 ML of adsorbed oxygen, 1159 K for 1.0 ML oxygen, and 1182 K for 1.2 ML. The worst case error for T_g, estimated using twice the standard error from the least squares fit, was 1000–1360 K (172–234 meV) for the 0.5 ML data.

Fig. 3 shows TOF spectra for O_2 desorbing after depositing oxygen with an NO_2 beam. The total quantity of ad- and absorbed oxygen was 0.9 ML for the spectrum in Fig. 3a and 1.5 ML for the spectrum in Fig. 3b. These coverages straddle the coverages from O_2 dosing shown in Figs. 2b and 2c, but the fitted values of T_g are nearly identical, 1176 and 1170 K, respectively.

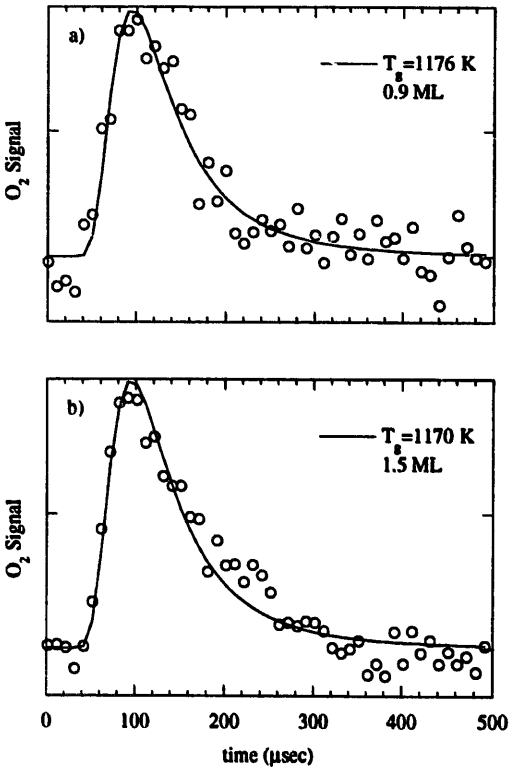

Fig. 3. Deconvoluted O_2 TOF spectra (circles) and least squares fits (lines) for varying amounts of ad- and absorbed oxygen, all taken after NO_2 dosing.

4. Discussion and conclusions

The TOF spectra shown in Figs. 2 and 3 are essentially the same, regardless of the initial oxygen dose or source of oxygen, and can be described by Maxwell–Boltzmann velocity distributions with $T_g \approx 1175$ K. It is important to note that independent fits to each desorption TOF spectrum of Figs. 2 and 3 gave the same result, with T_g varying from 1170 to 1182 K. Even if the data are not exactly fit by Maxwell–Boltzmann velocity distributions, the close similarity of the results still strongly suggests that the velocity distributions are the same.

That all of the velocity distributions are identical within the precision of our measurements indicates that the mechanism for the desorption of recombinatively formed O_2 from ad- and absorbed oxygen is the same. There are at least two possibilities for the similarity. One is that the absorbed oxygen segregates to the surface, where it first equilibrates, recombines, and then desorbs. The other is that there is some difference between the recombination of initially ad- and absorbed oxygen, but that the recombined oxygen is trapped or adsorbed on the surface before desorption occurs. It is important to note that the TOF spectra are the same even though the TPD spectra are quite different. This is especially true for the results from NO_2 and O_2 dosing, where the difference in the TPD spectra indicates either a difference in where, and at what local concentrations, oxygen is absorbed, or the presence of some co-absorbed or co-adsorbed nitrogen.

Another aspect of the data is that T_g, the temperature of the desorbing gas, is noticeably hotter than the surface temperature. This is most clearly shown for the experiments with sub-surface oxygen, where most of the O_2 desorbed in a narrow temperature range at surface temperatures between 800 and 900 K, as shown by the dashed lines in Figs. 2b and 2c. It is also true for saturation coverage of the overlayer, 0.5 ML, shown in Fig. 2a. The dashed line is an approximation to the expected TOF spectrum if the desorbing O_2 were to come off at the surface temperature. This was derived by dividing the 0.5 ML TPD spectrum into six segments from 650 to 1250 K, each 100 K long. TOF spectra were calculated using the temperature at the midpoint of each segment for T_g, and then added together, weighted by the relative intensity of each segment in the TPD spectrum. The result is much cooler than the measured spectrum (it is close to a Maxwell–Boltzmann velocity distribution with $T_g = 900$ K), with the leading edge of the experimental distribution clearly faster than that of the calculated surface-thermalized distribution. One possibility to explain this result is a potential barrier between oxygen on the surface and in the gas phase, best investigated by molecular beam sticking experiments.

In conclusion, we have measured the velocity distributions of desorbing oxygen originating from the surface and sub-surface regions of Rh(111). The results are well represented by *identical* Maxwell–Boltzmann velocity distributions, significantly hotter than the surface temperature. We conclude that surface and sub-surface oxygen share a common dynamical state prior to desorption.

Acknowledgements

Acknowledgement is made to the donors of The Petroleum Research Fund, administered by the ACS, for partial support of this research. This work was also supported in part by the Materials Research Science and Engineering Center Program of the National Science Foundation under award DMR-9400379. J.I.C. also thanks AT&T Bell Laboratories for financial support through the Graduate Research Program for Women.

References

[1] C.T. Reimann, M. El-Maazawi, K. Walzl, B.J. Garrison, N. Winograd and D.M. Deaven, J. Chem. Phys. 90 (1989) 2027.
[2] X. Xu and C.M. Friend, J. Am. Chem. Soc. 113 (1991) 6779.
[3] K.A. Peterlinz and S.J. Sibener, J. Phys. Chem. 99 (1995) 2817.
[4] K.A. Peterlinz and S.J. Sibener, Surf. Sci., submitted.
[5] J.I. Colonell and K.D. Gibson, unpublished result.
[6] P.A. Thiel, J.T. Yates, Jr. and W.H. Weinberg, Surf. Sci. 82 (1979) 22.
[7] G. Comsa, R. David and B.-J. Schumacher, Surf. Sci. 85 (1979) 45.
[8] G. Comsa and R. David, Surf. Sci. 117 (1982) 77.
[9] G. Anger, A. Winkler and K.D. Rendulic, Surf. Sci. 220 (1989) 1.
[10] H.A. Michelsen and D.J. Auerbach, J. Chem. Phys. 94 (1991) 7502.
[11] K.D. Rendulic, G. Anger and A. Winkler, Surf. Sci. 208 (1989) 404.
[12] H.P. Steinrück, K.D. Rendulic and A. Winkler, Surf. Sci. 154 (1985) 99.
[13] A.D. Johnson, K.J. Maynard, S.P. Daley, Q.Y. Yang and S.T. Ceyer, Phys. Rev. Lett. 67 (1991) 927.
[14] A.D. Johnson, S.P. Daley, A.L. Utz and S.T. Ceyer, Science 257 (1992) 223.
[15] S.P. Daley, A.L. Utz, T.R. Trautman and S.T. Ceyer, J. Am. Chem. Soc. 116 (1994) 6001.
[16] D.F. Padowitz and S.J. Sibener, Surf. Sci. 254 (1991) 125.
[17] J.I. Colonell, K.D. Gibson and S.J. Sibener, J. Chem. Phys., submitted.
[18] L. Bugyi and F. Solymosi, Surf. Sci. 188 (1987) 475.
[19] L.A. DeLouise and N. Winograd, Surf. Sci. 159 (1985) 199.
[20] T.W. Root, L.D. Schmidt and G.B. Fisher, Surf. Sci. 134 (1983) 30.
[21] L. Bugyi and F. Solymosi, Surf. Sci. 258 (1991) 55.